Inorg. Chem. **2006**, *45*, 255–262

Self-Assembly of a Tetranuclear Ni_4 Cluster with an $S = 4$ Ground State: The First 3d Metal Cluster Bearing a μ_4-η^2:η^2-O,O Carbonate Ligand

Matilde Fondo,*,† Noelia Ocampo,† Ana M. García-Deibe,† Ramón Vicente,‡ Montserrat Corbella,‡ Manuel R. Bermejo,§ and Jesús Sanmartín§

Departamento de Química Inorgánica, Facultade de Ciencias, Universidade de Santiago de Compostela, E-27002 Lugo, Spain, Departament de Química Inorgànica, Facultat de Química, Universitat de Barcelona, E-08028 Barcelona, Spain, and Departamento de Química Inorgánica, Facultade de Química, Universidade de Santiago de Compostela, E-15782 Santiago de Compostela, Spain

Received July 18, 2005

Reaction of nickel(II) acetate with H_3L (2-(5-bromo-2-hydroxyphenyl)-1,3-bis[4-(5-bromo-2-hydroxyphenyl)-3-azabut-3-enyl]-1,3-imidazolidine) yields $[Ni_2L(OAc)(H_2O)_2]\cdot 3MeCN\cdot 2H_2O$ (**1**·3MeCN·2H_2O), crystallographically characterized. **1** is unstable in solution for a long time and hydrolyzes to give $[Ni_2L(o\text{-}OC_6H_3BrCHO)(H_2O)]\cdot 2.25MeCN\cdot H_2O$ (**2**·2.25MeCN·H_2O). In addition, **1** uptakes CO_2 from air in a basic methanol/acetonitrile solution, yielding $\{[Ni_2L(MeOH)]_2(CO_3)\}\cdot 1.5MeOH\cdot MeCN\cdot H_2O$ (**3**·1.5MeOH·MeCN·H_2O). The X-ray characterization of **3** reveals that it is a tetranuclear nickel cluster, which can be considered as the result of a self-assembly process from two dinuclear $[Ni_2L]^+$ blocks, joined by a μ_4-η^2:η^2-O,O carbonate ligand. The coordination mode of the carbonate anion is highly unusual and, to the best of our knowledge, it has not been described thus far for first-row transition metal complexes or magnetically studied until now. Magnetic characterization of **1** and **3** shows net intramolecular ferromagnetic coupling between the metal atoms in both cases, with $S = 2$ and $S = 4$ ground states for **1** and **3**, respectively.

Introduction

Polynuclear 3d metal complexes with unpaired electrons in their spin ground state are considered promising compounds for the design of new magnetic materials, with special attention focused in the search for molecular-based magnets or nanomagnets.[1−5] The essential prerequisite of such work is to prepare molecular species with large spin ground states, and the usual strategy is to generate ferromagnetic interactions between unpaired spin centers. Therefore, the development of methods for the preparation of polynuclear complexes of targeted topology and a predefined number of metal atoms is an essential step for the investigation of this phenomenon. The self-assembly of first-row transition metals and suitable bridging ligands has proved to be a very powerful approach for well-defined arrangements of metal ions.[6−9] However, even with controlling the number and

* To whom correspondence should be addressed. E-mail: qimatf69@usc.es.

† Departamento de Química Inorgánica, Facultade de Ciencias, Universidade de Santiago de Compostela.

‡ Departament de Química Inorgànica, Universitat de Barcelona.

§ Departamento de Química Inorgánica, Facultade de Química, Universidade de Santiago de Compostela.

(1) Kahn, O. *Angew. Chem., Int. Ed. Engl.* **1985**, *24*, 834.

(2) *Magnetism: Molecules to Materials, II; Molecule-Based Materials*; Miller. J. S., Drillon, M., Eds.; Wiley-VCH: Weinheim, Germany, 2001.

(3) (a) Sessoli, R.; Tsai, H.-L.; Schake, A. R.; Wang, S.; Vincent, J. B.; Folting, K.; Gatteschi, D.; Christou, G.; Hendrickson, D. N. *J. Am. Chem. Soc.* **1993**, *115*, 1804. (b) Castro, S. L.; Sun, Z.; Grant, C. M.; Bollinger, J. C.; Hendrickson, D. N.; Christou, G. *J. Am. Chem. Soc.* **1998**, *120*, 2365. (c) Gatteschi, D.; Sessoli, R.; Cornia, A. *Chem. Commun.* **2000**, 725.

(4) (a) Larionova, J.; Gross, M.; Pilkington, M.; Andres, H.; Stoeckli-Evans, H.; Güdel, H. U.; Decurtins, S. *Angew. Chem., Int. Ed.* **2000**, *39*, 1605. (b) Ochsenbein, S. T.; Murrie, M.; Rusanov, E.; Stoeckli-Evans, H.; Sekine, C.; Güdel, H. U. *Inorg. Chem.* **2002**, *41*, 5133.

(5) (a) Cadiou, C.; Murrie, M.; Paulsen, C.; Villar, V.; Wernsdorfer, W.; Winpenny, R. E. P. *Chem. Commun.* **2001**, 2666. (b) Andres, H.; Basler, R.; Blake, A. J.; Cadiou, C.; Chaboussant, G.; Grant, G. M.; Güdel, H. U.; Murrie, M.; Parsons, S.; Paulsen, C.; Semadini, F.; Villar, V.; Wernsdorfer, W.; Winpenny, R. E. P. *Chem.−Eur. J.* **2002**, *8*, 4867.

(6) Lehn, J. M. *Supramolecular Chemistry: Concepts and Perspectives*; Wiley-VCH: Weinheim, Germany, 1995.

10.1021/ic051194s CCC: $33.50
Published on Web 12/06/2005

Scheme 1

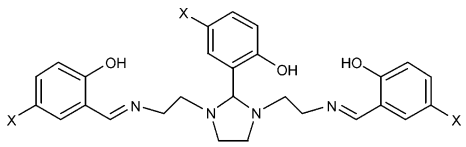

geometry of the metal centers in a predefined complex, the type of magnetic exchange interaction between the metal ions is difficult to predict.

We have recently reported that a bidentate compartmental Schiff base generates dinuclear copper complexes of stoichiometry $[Cu_2L^1X]$ [X = external bridging ligand, H_3L^1 in Scheme 1],[10] with intramolecular ferromagnetic coupling, independently of the exogenous bridge. Therefore, it seems that this Schiff base can give rise to dinuclear compounds with a predefined ground state. In fact, density functional theory (DFT) calculations demonstrated that the Schiff base provides an NCN bridge between the metal ions that helps to mediate the ferromagnetic exchange.[11] Consequently, the use of suitable cross-linking ligands between the dinuclear units could be a route to produce complexes of higher nuclearity, with all of the unpaired electrons aligned parallel to each other.

In addition, our experience with this kind of complex shows that dinuclear compounds can be easily converted into tetranuclear ones by reaction with CO_2 from air in a basic medium[11,12] in a self-assembly process. With these considerations in mind, we have synthesized a dinuclear nickel complex $[Ni_2L(OAc)]$ (H_3L in Scheme 1) as a precursor, with an $S = 2$ ground state, as predicted. Its stability and reactivity in a basic medium was investigated, in the hope of isolating the corresponding $[(Ni_2L)_2CO_3]$ tetranuclear compound with an $S = 4$ ground state. The results achieved are reported herein.

Experimental Section

General Considerations. Elemental analyses of C, H, and N were performed on a Carlo Erba EA 1108 analyzer. Infrared spectra were recorded as KBr pellets on a Bio-Rad FTS 135 spectrophotometer in the range 4000−600 cm^{-1}. Electrospray mass spectra were obtained on a Hewlett-Packard LC/MS spectrometer, with methanol as the solvent.

Syntheses. H_3L has been synthesized following a method previously described[12b] and satisfactorily characterized by elemental analysis, mass spectrometry, and IR and ^1H NMR spectroscopies. All solvents, $Ni(OAc)_2{\cdot}4H_2O$, and tetramethylammonium hydroxide pentahydrate are commercially available and were used without further purification.

$Ni_2L(OAc)(H_2O)_4$ (1·2H_2O). $Ni(OAc)_2{\cdot}4H_2O$ (0.11 g, 0.44 mmol) was added to a methanol/acetonitrile solution (40 mL) of H_3L (0.15 g, 0.22 mmol). The mixture was stirred in air for 6 h, and the resultant solution was left to slowly evaporate (3 days) until light-green crystals of $[Ni_2L(OAc)(H_2O)_2]{\cdot}3MeCN{\cdot}2H_2O$ (**1**·3MeCN·2H_2O), suitable for X-ray diffraction studies, precipitated. The crystals were filtered off and dried in air to collect a green crystalline sample. Its elemental analysis is in agreement with the proposed stoichiometry $Ni_2L(OAc)(H_2O)_4$, indicating that the complex loses the most volatile solvent on drying (0.12 g, 58.1%), mp > 300 °C. Found: C 36.67; H 3.24; N 5.90. $C_{29}Br_3H_{38}N_4O_{11}Ni_2$ requires: C, 37.00; H, 3.70; N, 5.95. MS (ES): *m*/*z* 808.8 $[Ni_2L]^+$. IR (KBr, ν/cm^{-1}): 1641 (C═N), 3419 (OH).

When **1**·2H_2O is dissolved in methanol and the dilute solution is left to slowly evaporate (four weeks), few single crystals of $[Ni_2L(o\text{-}OC_6H_3BrCHO)(H_2O)]{\cdot}2.25MeCN{\cdot}H_2O$ (**2**·2.25MeCN·H_2O), suitable for X-ray diffraction studies, are isolated.

{$[Ni_2L(MeOH)]_2(CO_3)$}·1.5MeOH·MeCN·H_2O (3·1.5MeOH·MeCN·H_2O). Tetramethylammonium hydroxide pentahydrate (0.038 g, 0.21 mmol) was added to a methanol/acetonitrile solution (40 mL) of **1**·2H_2O (0.200 g, 0.21 mmol). The mixture was stirred in air for 8 h, and the resultant solution was left to slowly evaporate until green crystals of **3**·1.5MeOH·MeCN·H_2O, suitable for X-ray diffraction studies, precipitated. The solid was filtered off and dried in air. Elemental analysis of the bulk sample is in agreement with the proposed stoichiometry $(Ni_2L)_2(CO_3)(MeOH)_{3.5}(MeCN)(H_2O)$ (0.142 g, 36.5%), mp > 300 °C. Found: C 39.12; H 3.60; N 6.84. $C_{60.5}Br_6H_{67}N_9O_{13.5}Ni_4$ requires: C, 39.20; H, 3.60; N, 6.80. MS (ES): *m*/*z* 808.8 $[Ni_2L]^+$. IR (KBr, ν/cm^{-1}): 1521, 1382 (CO_3), 1640 (C═N), 3390 (OH_2).

X-ray Structure Determinations. Single crystals of **1**·3MeCN·2H_2O, **2**·2.25MeCN·H_2O, and **3**·1.5MeOH·MeCN·H_2O were obtained as detailed above. Diffraction data were collected at 120 K, using a Bruker SMART CCD-1000 diffractometer employing graphite-monochromated Mo Kα radiation ($\lambda = 0.71073$ Å) for **1**·3MeCN·2H_2O and **3**·1.5MeOH·MeCN·H_2O and a Bruker Nonius FR591-Kappa CCD2000 diffractometer employing Cu Kα radiation ($\lambda = 1.54180$ Å) monochromated with a multilayer graded mirror for **2**·2.25MeCN·H_2O. No significant decays were observed, and data were corrected for Lorentz and polarization effects. Multiscan absorption corrections were applied using SADABS (**1**·3MeCN·2H_2O and **3**·1.5MeOH·MeCN·H_2O) or SORTAV (**2**·2.25MeCN·H_2O).[13] The structures were solved by standard direct methods, employing DIRDIF (**1**·3MeCN·2H_2O), SIR-92 (**2**·2.25MeCN·H_2O), or SHELXS-97 (**3**·1.5MeOH·MeCN·H_2O),[14] and refined by Fourier techniques based on F^2 using SHELXL-97.[14c] Non-hydrogen atoms were anisotropically refined, except for some of those corresponding solvated molecules that were isotropically treated. Hydrogen atoms of organic groups were included at geometrically calculated

(7) Saalfrank, R. W.; Demleitner, B. In *Perspectives in Supramolecular Chemistry*; Sauvage, J. P., Ed.; Wiley-VCH: Weinheim, 1999; Vol. 5, pp 1−51.
(8) Swiegers, G. F.; Malafetse, T. J. *Coord. Chem. Rev.* **2002**, *225*, 91.
(9) Yeh, R. H.; Davis, A. V.; Raymond, K. N. *Compr. Coord. Chem. II* **2004**, *7*, 327.
(10) (a) Fondo, M.; García-Deibe, A. M.; Sanmartín, J.; Bermejo, M. R.; Lezama, L.; Rojo, T. *Eur. J. Inorg. Chem.* **2003**, 3703. (b) Fondo, M.; García-Deibe, A. M.; Corbella, M.; Ribas, J.; Llamas-Saiz, A.; Bermejo, M. R.; Sanmartín, J. *Dalton Trans.* **2004**, 3503.
(11) Fondo, M.; García-Deibe, A. M.; Corbella, M.; Ruiz, E.; Tercero, J.; Sanmartín, J.; Bermejo, M. R. *Inorg. Chem.* **2005**, *44*, 5011.
(12) (a) Fondo, M.; García-Deibe, A. M.; Bermejo, M. R.; Sanmartín, J.; Llamas-Saiz, A. L. *J. Chem. Soc., Dalton Trans.* **2002**, 4746. (b) Fondo, M.; García-Deibe, A. M.; Ocampo, N.; Sanmartín, J.; Bermejo, M. R. *Dalton Trans.* **2004**, 2135.
(13) (a) S*ADABS, Area-Detector Absorption Correction*; Siemens Industrial Automation Inc.: Madison, WI, 1996. (b) Blessing, R. H.; *Acta Crystallogr., Sect. A: Found. Crystallogr.* **1995**, *51*, 33.
(14) (a) SIR92 A Program for Crystal Structure Solution. Altomare, A.; Cascarano, G.; Giacovazzo, C.; Guagliardi, A. *J. Appl. Crystallogr.* **1993**, *26*, 343. (b) Beurskens, P. T.; Beurskens, G.; Bosman, W. P.; de Gelder, R.; Garcia-Granda, S.; Gould, R. O.; Israel, R.; Smits, J. M. M. *DIRDIF96 Program System*; Crystallography Laboratory, University of Nijmegen: The Netherlands, 1996. (c) Sheldrick, G. M. *SHELX97 Programs for Crystal Structure Analysis*; Institüt für Anorganische Chemie der Universität: Göttingen, Germany, 1998.

Scheme 2

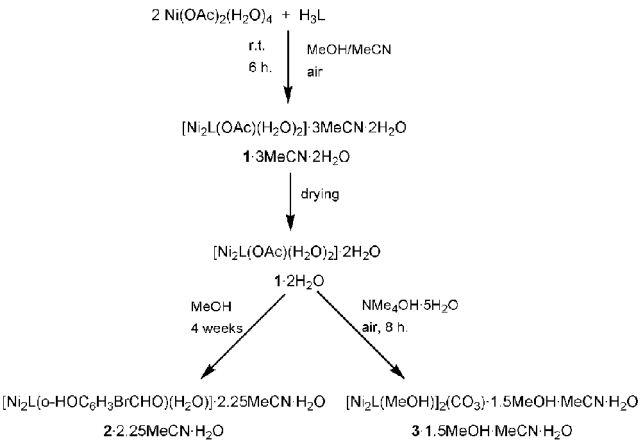

positions, with thermal parameters derived from the parent atoms. H atoms attached to water molecules could be located on Fourier maps. In the case of **1**·3MeCN·2H_2O and **3**·1.5MeOH·MeCN·H_2O, the coordinates of H atoms attached to water molecules were fixed and given isotropic displacement parameters of 0.1 and 0.08 Å^2, respectively, whereas in the case of **2**·2.25MeCN·H_2O, H-atom coordinates could be refined and isotropically treated. At the end of the refinements, the higher electron density maxima and minima and holes were located in the Fourier maps close to Br atoms.

Magnetic Measurements. Magnetic susceptibility measurements for powdered crystalline samples of **1**·2H_2O and **3**·1.5MeOH·MeCN·H_2O were carried out at the Servei de Magnetoquímica of the Universitat de Barcelona with a Quantum Design Squid MPMS-XL susceptometer. The measurements were performed in the temperature range of 2−300 K under magnetic fields of 10 000 G (2−300 K) for **1**·2H_2O and 7000 G (2−300 K) for **3**·1.5MeOH·MeCN·H_2O. The fit for compound **1**·2H_2O was performed minimizing the function $R = \Sigma(\chi_M T_{exp} - \chi_M T_{cal})^2/\Sigma(\chi_M T_{exp})^2$. Magnetic fields ranging from 0 to 50 000 G were used for magnetization measurements at 2 K. Diamagnetic corrections were estimated from Pascal's Tables.

Results and Discussion

Syntheses. The reaction of Ni(OAc)$_2$·4H_2O with H_3L in methanol/acetonitrile yields [$Ni_2L(OAc)(H_2O)_2$]·3MeCN·2H_2O (**1**·3MeCN·2H_2O) as single crystals. The complex loses the most volatile solvent upon drying to give a crystalline sample of [$Ni_2L(OAc)(H_2O)_2$]·2H_2O (**1**·2H_2O). Its stability and reactivity in a basic medium was investigated (Scheme 2). Accordingly, when a dilute methanol solution of **1**·2H_2O is left to stand for 4 weeks, few single crystals of [Ni_2L(*o*-OC_6H_4BrCHO)(H_2O)]·2.25MeCN·H_2O (**2**·2.25MeCN·H_2O) are isolated and the complex is crystallographically characterized. The presence of the aldehyde ligand demonstrates that **1** is unstable in solution for a long time, with the Schiff base undergoing hydrolysis. In addition, the reaction of **1**·2H_2O with NMe_4OH·5H_2O in air gave {[$Ni_2L(MeOH)]_2$(CO_3)}·1.5MeOH·MeCN·H_2O (**3**·1.5MeOH·MeCN·H_2O). The presence of a carbonate ligand in the crystal structure of **3** indicates that **1**·2H_2O can act as a carbon dioxide scrubber in a basic medium, removing CO_2 from air. This reaction is not without precedent, as it is well-known that several nickel(II) complexes can spontaneously absorb carbon dioxide to convert it into carbonate.[15−17]

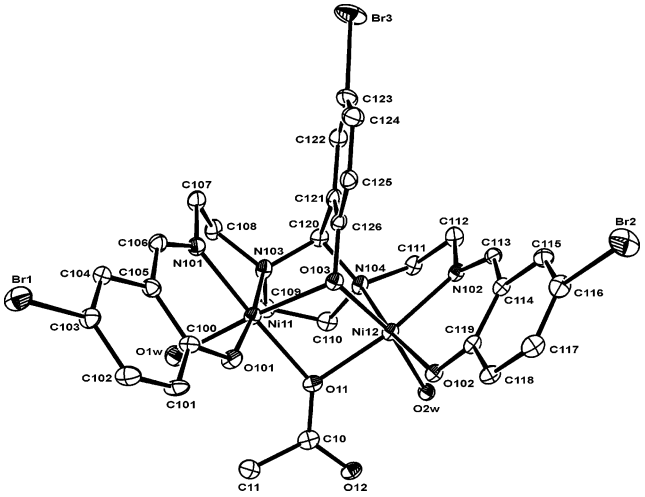

Figure 1. ORTEP view of the crystal structure of **1**. Hydrogen atoms are omitted for clarity.

Complexes **1**−**3** were crystallographically characterized. The small quantity of crystals obtained for **2**·2.25MeCN·H_2O prevented its further characterization. Compounds **1**·2H_2O and **3**·1.5MeOH·MeCN·H_2O were additionally studied by spectroscopic, spectrometric, and analytical methods as well as by magnetic measurements.

The infrared spectra of **1**·2H_2O and **3**·1.5MeOH·MeCN·H_2O contain a sharp band at ca. 1640 cm^{-1}, in agreement with the coordination of the Schiff base to the metal ions through the imine nitrogen atoms. Additionally, a wide band centered at ca. 3400 cm^{-1} agrees with the hydration of both complexes. **3** shows two additional sharp bands at 1536 and 1344 cm^{-1}, consistent with the presence of the carbonate ligand.[11,12] The ESI mass spectra show the existence of dinuclear units in solution, with a peak at 808.8 (100%) *m*/*z* in both cases corresponding to $[Ni_2L]^+$ fragments. However, no peaks related to the whole molecules could be observed in any of the spectra, probably due to their neutral nature.

Description of the Crystal Structures

[$Ni_2L(OAc)(H_2O)_2$]·3MeCN·2H_2O (1·3MeCN·2H_2O). An ORTEP view of **1** is shown in Figure 1. Experimental details are given in Table 1, and main distances and angles are listed in Table 2.

The crystal structure shows that **1**·3MeCN·2H_2O contains [$Ni_2L(OAc)(H_2O)_2$] molecules in the unit cell and water and acetonitrile as solvates. **1** is a neutral dinuclear compound, where the L^{3-} Schiff base acts as a compartmental trianionic heptadentate ligand, using each one of its N_2O compartments to coordinate a nickel atom. Thus, the metal atoms are joined

(15) Kitajima, N.; Hikichi, S.; Tanaka, M.; Moro-oka, Y. *J. Am. Chem. Soc*. **1993**, *115*, 5496.
(16) (a) Escuer, A.; Vicente, R.; Kumar, S. B.; Solans, X.; Font-Bardía, M.; Caneschi, A. *Inorg. Chem.* **1996**, *35*, 3094. (b) Escuer, A.; Vicente, R.; Kumar, S. B.; Mautner, F. A. *J. Chem. Soc., Dalton Trans.* **1998**, 3473. (c) Escuer, A.; Mautner, F. A.; Peñalba, E.; Vicente, R. *Inorg. Chem.* **1998**, *37*, 4190.
(17) Dussart, Y.; Harding, C.; Dalgaard, P.; McKenzie, C.; Kadirvelraj, R.; McKee, V.; Nelson, J. *J. Chem. Soc., Dalton Trans.* **2002**, 1704.

Table 1. Crystal Data and Structure Refinement Parameters for **1**·3MeCN·2H_2O, **2**·2.25MeCN·H_2O, and **3**·1.5MeOH·MeCN·H_2O

	1·3MeCN·2H_2O	**2**·2.25MeCN·H_2O	**3**·1.5MeOH·MeCN·H_2O
empirical formula	$C_{35}H_{42}N_7O_9Br_3Ni_2$	$C_{38.50}H_{38.75}Br_4N_{6.25}Ni_2O_7$	$C_{60.50}H_{67}N_9O_{13.50}Br_6Ni_4$
formula weight	1061.91	1138.07	1850.53
crystal system	monoclinic	orthorhombic	triclinic
space group	*I*2/*a*	*Pbna*	$P\bar{1}$
temperature, K	120 (2)	120 (2)	120 (2)
a, Å	15.177(3)	14.6160(11)	12.7152 (11)
b, Å	19.091(4)	24.349(2)	12.7462 (11)
c, Å	29.883(7)	24.4841(13)	23.427 (2)
α, deg	90	90.00	77.946 (2)
β, deg	97.829(14)	90.00	84.651 (2)
γ, deg	90	90.00	68.156 (2)
V, Å^3	8578(3)	8713.5(12)	3466.0 (5)
Z	8	8	2
μ, mm^{-1}	3.730	5.869	4.622
reflns collected	37987	87978	58267
independent reflns	7317 [R_{int} = 0.0570]	7417 [R_{int} = 0.0915]	14090 [R_{int} = 0.0386]
data/restraints/params	7317/7/478	7417/0/543	14090/0/846
final R index [$I > 2\sigma(I)$]	R1 = 0.0520 wR2 = 0.1273	R1 = 0.0495 wR2 = 0.1318	R1 = 0.0434, wR2 = 0.0950
R indices [all data]	R1 = 0.0906, wR2 = 0.1520	R1 = 0.0578 wR2= 0.1403	R1 = 0.0875, wR2 = 0.1176

Table 2. Selected Bond Lengths [Å] and Angles [deg] for **1**·3MeCN·2H_2O

Ni(11)−O(101)	1.988(4)	Ni(12)−N(102)	2.014(5)
Ni(11)−N(101)	2.029(6)	Ni(12)−O(102)	2.045(4)
Ni(11)−O(103)	2.070(4)	Ni(12)−O(103)	2.071(4)
Ni(11)−O(11)	2.105(4)	Ni(12)−O(11)	2.106(5)
Ni(11)−N(103)	2.141(5)	Ni(12)−O(2W)	2.119(4)
Ni(11)−O(1W)	2.174(5)	Ni(12)−N(104)	2.142(5)
Ni(11)···Ni(12)	3.1614(14)		

N(101)−Ni(11)−O(11)	177.5(2)	N(102)−Ni(12)−O(11)	171.63(19)
O(101)−Ni(11)−N(103)	173.8(2)	O(102)−Ni(12)−N(104)	171.08(19)
O(103)−Ni(11)−O(1W)	173.54(19)	O(103)−Ni(12)−O(2W)	166.54(17)
Ni(11)−O(103)−Ni(12)	99.53(18)	Ni(11)−O(11)−Ni(12)	97.29(18)

Table 3. Selected Bond Lengths [Å] and Angles [deg] for **2**·2.25MeCN·H_2O

Ni(11)−O(101)	1.999(3)	Ni(12)−O(102)	2.000(3)
Ni(11)−N(101)	2.013(4)	Ni(12)−N(102)	2.006(3)
Ni(11)−O(11)	2.015(3)	Ni(12)−O(11)	2.071(3)
Ni(11)−O(103)	2.073(3)	Ni(12)−O(103)	2.090(3)
Ni(11)−O(12)	2.119(3)	Ni(12)−O(12W)	2.139(4)
Ni(11)−N(103)	2.154(4)	Ni(12)−N(104)	2.172(3)
Ni(11)···Ni(12)	3.0925(11)		

O(103)−Ni(11)−O(12)	168.50(12)	O(103)−Ni(12)−O(12W)	172.92(13)
O(101)−Ni(11)−N(103)	173.20(13)	O(102)−Ni(12)−N(104)	174.47(13)
N(101)−Ni(11)−O(11)	176.74(14)	N(102)−Ni(12)−O(11)	174.87(13)
Ni(11)−O(103)−Ni(12)	95.93(12)	Ni(11)−O(11)−Ni(12)	98.38(12)

to one terminal phenol oxygen (O101, O102), an iminic nitrogen (N101, N102), and an aminic nitrogen atom (N103, N104), with the aminic NCN group (N103−C120−N104) acting as a bridge between both nickel ions. In addition, the nickel centers are linked by the endogenous phenolate oxygen atom (O103) of the central ligand arm and by an exogenous bridging monodentate acetate group (O11). This gives rise to a nearly planar Ni_2O_2 metallacycle, with an intramolecular Ni···Ni distance of 3.1614(14) Å. The coordination spheres of the nickel atoms are completed by water molecules. Therefore, the metal centers are hexacoordinated in a N_2O_4 environment, with an octahedral geometry.

The Ni−O and Ni−N distances, as well as the angles about the metal atoms, show quite regular polyhedra around the central ions, with a Ni−O_{phenol}−Ni angle [99.53(18)°] slightly larger than that of the Ni−$O_{acetate}$−Ni bridge [97.29(18)°].

Finally, the water solvates form an intricate hydrogen bond scheme, contributing to the crystal packing. The acetonitrile solvent is weakly held in the unit cell, accounting for its removal upon drying. However, the number and kind of solvates present in the unit cell do not seem to significantly affect the structure of the metal complex, as we have previously demonstrated.[11,12a] Consequently, the structures of **1**·3MeCN·2H_2O and **1**·2H_2O should not significantly differ.

[Ni_2L(*o*-OC_6H_3BrCHO)(H_2O)]·2.25MeCN·H_2O (2·2.25-MeCN·H_2O). An ORTEP diagram of **2** is shown in Figure 2. Experimental details are given in Table 1, and main distances and angles are listed in Table 3.

The asymmetric unit of **2**·2.25MeCN·H_2O contains dinuclear [Ni_2L(*o*-OC_6H_3BrCHO)(H_2O)] neutral molecules and acetonitrile and water as solvates. The crystal structure of **2** resembles that of **1**. The Schiff base acts as heptadentate and trianionic, providing two N_2O compartments and a central phenol oxygen atom (O103), which bridges both metal ions. The main difference between **1** and **2** arises from the replacement of the initial acetate ligand by the anion of the substituted salicylaldehyde. The aldehyde ligand acts in a μ_2-η^2:η^1-O,O fashion, with the phenol oxygen atom bridging both nickel centers and the carbonyl oxygen atom

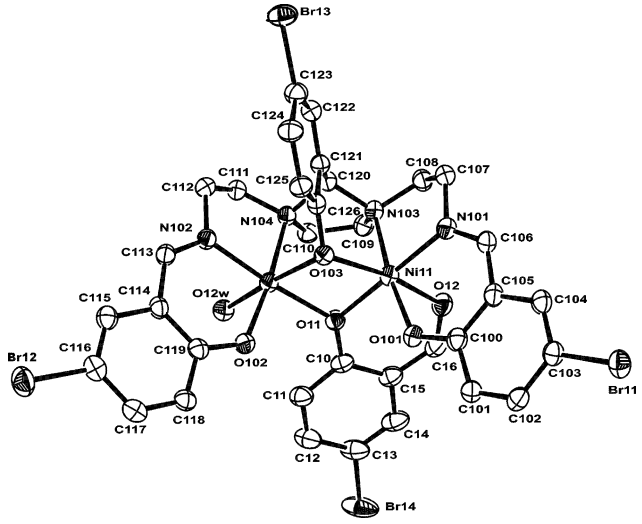

Figure 2. ORTEP view of the crystal structure of **2**. Hydrogen atoms are omitted for clarity.

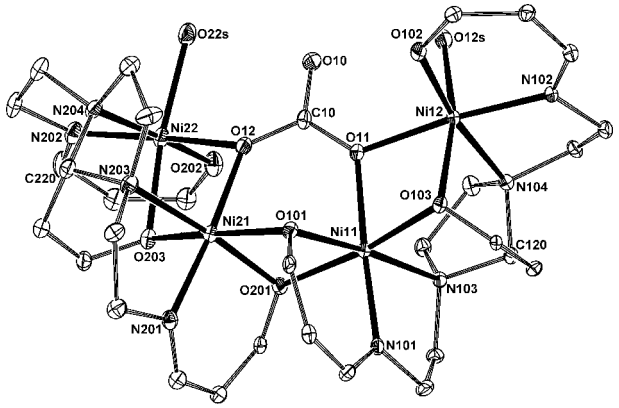

Figure 3. ORTEP view of the crystal structure of **3**. Due to the complexity of the structure, the bromine, some aromatic carbon, hydrogen atoms, and the labels of the carbon atoms have been omitted for clarity.

Table 4. Selected Bond Lengths [Å] and Angles [deg] for **3**·1.5MeOH·MeCN·H_2O

Ni(11)−N(101)	1.993(4)	Ni(21)−N(201)	2.004(5)
Ni(11)−O(101)	2.037(4)	Ni(21)−O(101)	2.171(4)
Ni(11)−O(201)	2.145(4)	Ni(21)−O(201)	1.993(4)
Ni(11)−N(103)	2.146(4)	Ni(21)−N(203)	2.147(5)
Ni(11)−O(11)	2.026(4)	Ni(21)−O(12)	2.024(4)
Ni(11)−O(103)	2.037(4)	Ni(21)−O(203)	2.053(4)
Ni(12)−N(102)	2.020(4)	Ni(22)−N(202)	1.996(5)
Ni(12)−O(102)	2.008(4)	Ni(22)−O(202)	2.001(4)
Ni(12)−O(12S)	2.128(4)	Ni(22)−O(22S)	2.080(4)
Ni(12)−N(104)	2.194(4)	Ni(22)−N(204)	2.165(5)
Ni(12)−O(103)	2.070(4)	Ni(22)−O(203)	2.049(4)
Ni(12)−O(11)	2.078(4)	Ni(22)−O(12)	2.065(4)
Ni(11)···Ni(12)	3.1003(11)	Ni(21)···Ni(22)	3.0205(10)
Ni(11)···Ni(21)	3.0109(11)	Ni(12)···Ni(22)	6.1036(12)
N(101)−Ni(11)−O(11)	176.74(15)	N(201)−Ni(21)−O(12)	175.00(17)
O(101)−Ni(11)−N(103)	175.40(16)	O(201)−Ni(21)−N(203)	175.07(17)
O(103)−Ni(11)−O(201)	172.91(14)	O(203)−Ni(21)−O(101)	170.35(14)
N(102)−Ni(12)−O(11)	173.64(16)	N(202)−Ni(22)−O(12)	172.28(17)
O(102)−Ni(12)−N(104)	171.39(16)	O(202)−Ni(22)−N(204)	173.47(17)
O(103)−Ni(12)−O(12S)	164.68(16)	O(203)−Ni(22)−O(22S)	169.56(16)
Ni(11)−O(103)−Ni(12)	98.05(15)	Ni(21)−O(203)−Ni(22)	94.84(16)
Ni(11)−O(11)−Ni(12)	98.11(15)	Ni(21)−O(12)−Ni(22)	95.21(16)
Ni(11)−O(101)−Ni(21)	91.30(14)	Ni(12)−O(11)−C(10)	131.0(3)
Ni(11)−O(201)−Ni(21)	93.30(15)	Ni(22)−O(12)−C(10)	127.4(0)

behaving as a terminal donor, bonded to Ni11 (Figure S1). The free coordination site on Ni12 is filled by one water molecule, and therefore, the symmetry of **2** is lowered with respect to **1**.

As a result, both nickel atoms are in N_2O_4 distorted octahedral environments, double bridged by two phenol oxygen atoms, as well as by the N103−C120−N104 moiety, at a Ni11···Ni12 distance of ca. 3.1 Å. The Ni−O−Ni angles are in the range 95−99°, with a shorter Ni−O_{phenol}−Ni angle in this case. The Ni−O11 and Ni−O103 distances reflect the slight asymmetry of both oxygen bridges. The remaining Ni−O and Ni−N distances, as well as the angles around the metal atoms, agree with the proposed geometry.

{[Ni_2L(MeOH)]$_2CO_3$}·1.5MeOH·MeCN·H_2O (3·1.5MeOH·MeCN·H_2O). Single crystals of **3**·1.5MeOH·MeCN·H_2O, suitable for X-ray diffraction studies, were grown as detailed in the Experimental Section. An ORTEP view of **3** is shown in Figure 3, and selected bond lengths and angles are shown in Table 4.

The structure of the complex can be understood as two dinuclear $[Ni_2L]^+$ units joined by a carbonate anion. In addition, two phenol oxygen atoms (O101, O201), provided by one terminal ligand arm of each Schiff base, link both $[Ni_2L]^+$ moieties. Thus, the tetranuclear complex can be considered to be obtained by the self-assembly of two dinuclear components. To simplify the crystal discussion, the dinuclear $[Ni_2L]^+$ moiety containing Ni11 and Ni12 should be called **3a** and the one containing Ni21 and Ni22, **3b** (see Scheme 3).

In each dinuclear cation, the compartmental trianionic $[L]^{3-}$ ligand acts as in **1** and **2**, using its N_2O tridentate cavities to coordinate a nickel ion and the central phenol oxygen atom (O*X*03, *X* = 1, 2) to bridge both metal centers. Up to now, the situation is the same as described in **1** and **2**. From now on, the ligand shows a behavior that has not been reported thus far for this type of Schiff base. Accordingly, the terminal phenol oxygen atom of one ligand arm (O101) of **3a** also links Ni21 in **3b** and vice versa, O201 from **3b** joins Ni11, belonging to **3a** (Scheme 3). At this point, O101 and O201 act as μ_2-η^2-O donors, whereas they behave as terminal donors in all of the complexes described herein and in the previous crystallographically solved compounds with this kind of ligand.[10−12,18−22] The coordination spheres of the nickel atoms are completed by two methanol molecules (O12S, O22S) from the solvent of crystallization and by an exogenous carbonate ligand, which also links both $[Ni_2L]^+$ cations (Scheme 3). The carbonate anion is acting in a μ_4-η^2:η^2-O,O fashion: one oxygen atom bridges the two metal centers of **3a** (Ni11, Ni12), the second one, the two nickel ions of the other dinuclear cation **3b** (Ni21, Ni22), whereas the third oxygen atom remains uncoordinated. This coordination mode of the carbonate ligand is quite unusual, and to the best of our knowledge, it has only been described for two previous related complexes,[23,24] none of them with first-row transition metals.

As a result, the nickel atoms are N_2O_4 hexacoordinated, with octahedral environments. The Ni−N and Ni−O distances, as well as the angles around the metal ions, agree with the proposed geometry and show the quite-regular polyhedra about the nickel atoms.

In accordance with the crystal discussion and to sum up, it could be useful to emphasize the number and nature of the bridging ligands between the nickel ions (Figure 4). Therefore, the pairs Ni11···Ni12 and Ni21···Ni22 are triple bridged by the N*X*03C*X*20N*X*04 (*X* = 1 or 2) moiety from

(18) Bailey, N. A.; McKenzie, E. D.; Worthington, J. M. *Inorg. Chim. Acta* **1977**, *25*, L137.
(19) Chiari, B.; Piovesana, O.; Tarantelli, T.; Zanelli, P. F. *Inorg. Chem.* **1983**, *22*, 2781.
(20) Yang, L.-W.; Liu, S.; Wong, E.; Rettig, S. J.; Orvig, C. *Inorg. Chem.* **1995**, *34*, 2164.
(21) (a) Copeland, E. P.; Ishenkumba, A. K.; Mague, J. T.; McPherson, G. L. *J. Chem. Soc., Dalton Trans.* **1997**, 2849. (b) Howell, R. C.; Spence, K. V. N.; Ishenkumba, A. K.; Williams, D. J. *J. Chem. Soc., Dalton Trans*. **1998**, 2727.
(22) Mukhopadhyay, U.; Govindasamy, L.; Ravikumar, K.; Velmurugan, D.; Ray, D. *Inorg. Chem. Commun*. **1998**, *1*, 152.
(23) (a) Carmona, E.; González, F.; Poveda, M. L.; Marín, J. M.; Atwood, J. L.; Rogers, R. D. *J. Am. Chem. Soc.* **1983**, *105*, 3365. (b) Alvarez, R.; Atwood, J. L.; Carmona, E.; Pérez, P. J.; Poveda, M. L.; Rogers, R. D. *Inorg. Chem.* **1991**, *30*, 1493.
(24) Matan, H. K.; Chang, S. C.; Ruble, J. R.; Black, I. N. L.; Stein, P. B. *Inorg. Chem*. **1993**, *32*, 4976.

Scheme 3

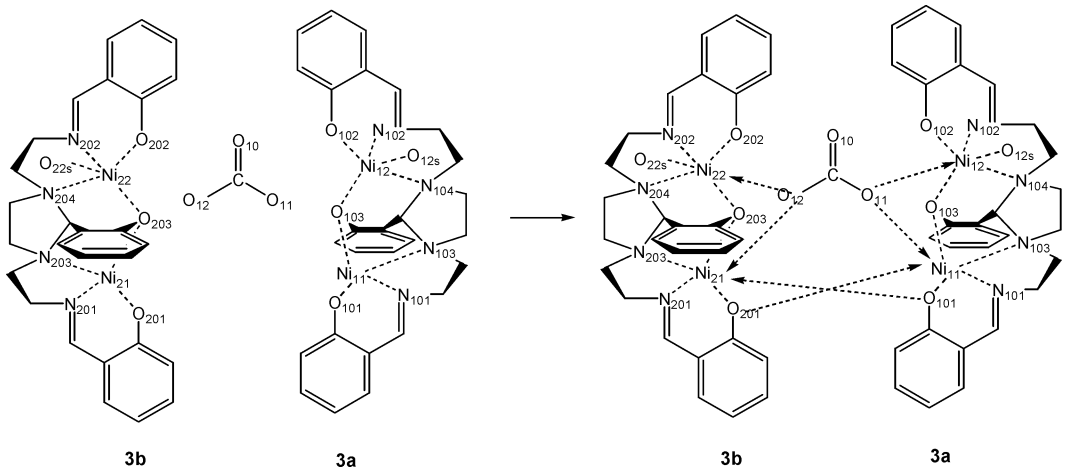

the Schiff base, the phenol oxygen atom of the central ligand arm (O*X*03) and one oxygen atom of the carbonate ligand (O11 or O12). The Ni−O*X*03 and Ni−O1*X* (*X* = 1 or 2) distances show the asymmetry of both phenol and carbonate bridges. This double oxygen bridge gives rise to a Ni_2O_2 metallacycle, with Ni···Ni distances of ca. 3.1 Å. However, despite the close similarity between both dinuclear fragments (**3a** and **3b**, Scheme 3), the Ni−O−Ni angles differ significantly. Thus, the Ni11−O−Ni12 angles are close to 98°, whereas the Ni21−O−Ni22 angles are significantly more acute (close to 95°).

The pair of atoms Ni11···Ni21 is also triple bridged, in this case by two phenol oxygen atoms and by the carbonate anion acting as a μ_2-η^1:η^1-O,O ligand in a syn−syn fashion. The Ni−O*X*01 (*X* = 1, 2) distances show the quite-high asymmetry of both Ni−O_{phenol}−Ni bridges (Ni11−O101−Ni21 and Ni11−O201−Ni21). These bridges also form a Ni_2O_2 metallacycle, with a Ni···Ni distance of 3.0109 Å, the shortest one found in **3**. In the same way, the Ni−O−Ni angles of this pair (ca. 91 and 93°) are the most acute of those described herein.

The Ni12 and Ni22 atoms are only bridged by the carbonate ligand, in an anti−anti mode, with a Ni12···Ni22 distance close to 6 Å. In addition, Ni11···Ni22 and Ni12···Ni21 are single bridged by the carbonate anion in a syn−anti fashion.

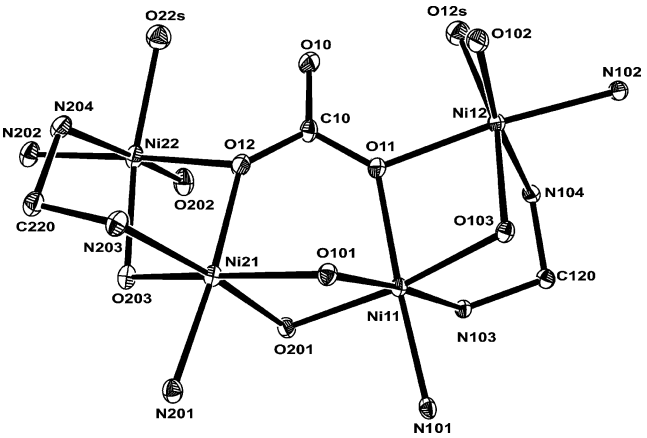

Figure 4. Core of **3** showing the bridging ligands between nickel atoms.

As a result of all of the crystallographic features described above, the four nickel atoms are on the vertexes of a distorted trapezoid, with three edges close to 3 Å and one close to 6 Å.

Magnetic Studies. The magnetic properties of **1**·2H_2O have been investigated in the 2−300 K temperature range, and a plot of $\chi_M T$ versus *T* is shown in Figure 5. The $\chi_M T$ product at 300 K (2.40 $cm^3\ mol^{-1}$ K) is on the order of the expected one for two uncoupled Ni(II) ions, with *g* about 2.2, and this value increases upon cooling to reach a maximum at 11 K (2.50 $cm^3\ mol^{-1}$ K), then diminishes with decreasing temperature. This behavior is consistent with ferromagnetically coupled dinuclear Ni(II) octahedral ions, with the decrease in $\chi_M T$ at low temperatures being attributed to either interdinuclear antiferromagnetic interactions and/or the effect of the zero-field splitting (ZFS) of the $S = 2$ ground state.

The experimental data were fitted with expression 1, derived from the Van Vleck formula ($H = -JS_1S_2$) for two $S = 1$ ions and modified for inclusion of the zero-field splitting parameter (*D*) in the ground state.

$$\chi_M T = \frac{Ng^2\beta^2}{3k} f(x) + \mathrm{TIP}T \qquad (1)$$

with

$$f(x) = \frac{2\,e^{-2J/kT} + 6\,e^{D/kT} + 24\,e^{-2D/kT}}{3\,e^{-2J/kT} + e^{-3J/kT} + e^{2D/kT} + 2\,e^{D/kT} + 2\,e^{-2D/kT}}$$

where the symbols have their usual meaning. The best least-squares fitting was obtained with $J = +3.6\ cm^{-1}$, $g = 2.14$, $D = 0.84\ cm^{-1}$, and TIP = $2.8 \times 10^{-4}\ cm^3\ mol^{-1}$ (R = 4.8×10^{-4}).

Attempts were made to compare this *J* value with those reported in the literature for complexes containing a Ni_2O_2 core to know if complex **1** follows a general pattern or deviates from the expected behavior. Some magneto−structural correlations for diphenoxo-bridged dinuclear nickel complexes were found[25,26] where the *J* value is related to

(25) Nanda, K. K.; Thompson, L. K.; Bridson, J. N.; Nag, K. *J. Chem. Soc., Chem. Commun.* **1994**, 1337.

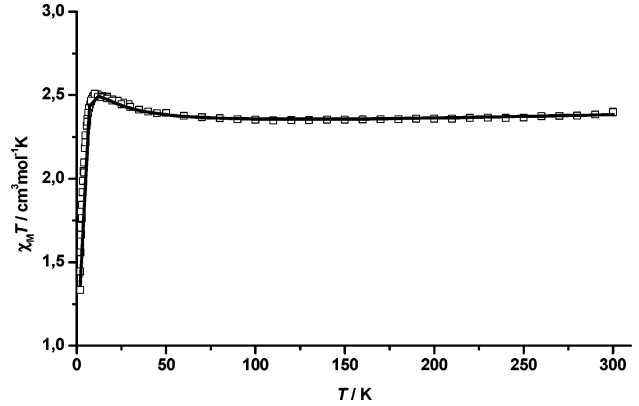

Figure 5. Plot of $\chi_M T$ vs T for **1**·2H_2O; scattered points: experimental results; dashed line: best fitting.

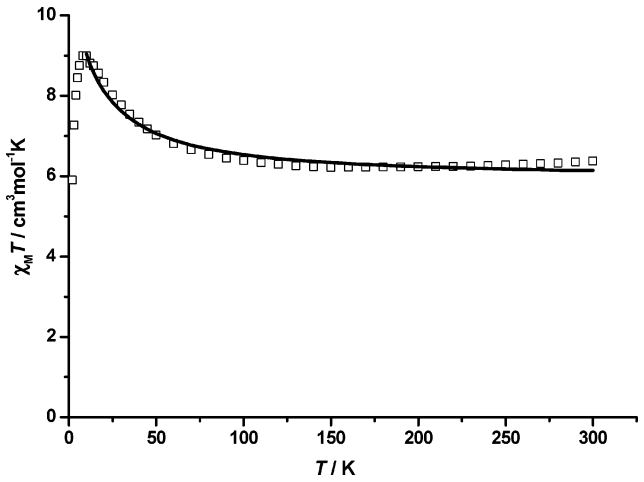

Figure 6. Plot of $\chi_M T$ vs T for **3**·1.5MeOH·MeCN·H_2O; scattered points: experimental results; dashed line: best fitting.

the Ni−O−Ni angle. In these correlations, the Ni_2O_2 core is in the *xy* plane, and the magnetic coupling becomes less antiferromagnetic as the Ni−O−Ni angle decreases, the accidental orthogonality occurring about 95°. In our case study, the average Ni−O−Ni angle is 98.4°, and we can reasonably expect antiferromagnetic coupling with a low $|J|$ value. Thus, the magnetic behavior of **1**·2H_2O seems to differ from the general pattern. However, this deviation is only apparent as, in addition to the O-bridges, this complex bears an NCN link [N103−C120−N104] between the metal ions, provided by the Schiff base, which contributes to mediate the ferromagnetic exchange.[11]

The variable temperature magnetic susceptibility data for **3** were recorded in the 2−300 K range. The $\chi_M T$ vs T plot (Figure 6) shows that the $\chi_M T$ value at 300 K is 6.3 cm^3 mol^{-1} K, and it increases as the temperature decreases, reaching a maximum of 9.0 cm^3 mol^{-1} K at 8 K. Then, the $\chi_M T$ product quickly decreases with diminishing temperature to a minimum of 5.9 cm ^{3}mol^{-1} K at 2 K. This behavior is characteristic of ferromagnetic coupling, the decreasing of the $\chi_M T$ value at low-temperature being attributed to zero-field splitting,[27] as it occurs in **1**.

The intramolecular ferromagnetic coupling seems to be confirmed by magnetization measurements at 2 K: this study shows that the reduced magnetization $M/N\beta$ varies linearly with low applied fields up to ca. 1 T and then progressively tends to 8.5, which points to an $S = 4$ ground state (Figure S2).

Several models were tested to explain the magnetic behavior of **3** on the basis of the structural data obtained by single X-ray diffraction studies. In a first approach, the interactions through the carbonate bridge were neglected, and a simple two J model (see *J1* and *J2* in Scheme 4) was tested using the computer CLUMAG program.[28] However, this model does not acceptably match the experimental data. This is in agreement with previous results published by us,[11] where DFT calculations demonstrate that the cross-link interactions through the carbonate bridge cannot be neglected, despite their small J values.

Therefore, a new model including the interactions through the carbonate ligand was considered. In view of the topology of the Ni_4 cluster, there are 6 possible exchange pathways, which can be grouped into four different exchange parameters J_1, J_2, J_3, and J_4 (Scheme 4). These correspond to the simultaneous μ_2-η^2-O(phenoxo), NCN, and oxo(carbonate) bridges between Ni(11)···Ni(12) and Ni(21)···Ni(22); the double μ_2-η^2-O(phenoxo) and μ_2-η^1:η^1-O,O carbonate bridges between Ni(11) and Ni(21); the anti−anti carbonate bridge between Ni(12)···Ni(22), and the syn−anti carbonate bridge between Ni(12)···Ni(21) and Ni(11)···Ni(22), respectively. As a consequence of the coupling scheme, the Hamiltonian to be used in the CLUMAG program[28] to fit the magnetic data in the 8−300 K temperature range is $H = -J_1(S_{11}S_{12} + S_{21}S_{22}) - J_2(S_{11}S_{21}) - J_3(S_{12}S_{22}) - J_4(S_{11}S_{22} + S_{12}S_{21})$. Because zero-field splitting was not taken into account, only data between 8 and 300 K were included in the fitting procedure.

Nevertheless, handling all of these interactions is difficult due to over-parametrization and correlation between the parameters. Therefore, some constraints should be included: as previously indicated, J_3 and J_4 should be small and their values were restricted between 2 and −2 cm^{-1}. A good fit of the experimental data gives parameters of $J_1 = 3.9$ cm^{-1}, $J_2 = 17.5$ cm^{-1}, $J_3 = -1.1$ cm^{-1}, $J_4 = -1.0$ cm^{-1}, $g = 2.43$, with an agreement factor $R = \Sigma(\chi_M T_{exp} - \chi_M T_{cal})^2/\Sigma(\chi_M T_{exp})^2$ of 3.79×10^{-4}. TIP was assumed as 6×10^{-4} cm^3 mol^{-1}, a typical value for Ni_4 complexes. These data are completely consistent with the expected results: J_1 should be positive, as the Schiff base provides an NCN bridge between the metal ions that contributes to mediate the ferromagnetic exchange.[11] In addition, it should be of the same order of magnitude as that found in **1** (3.6 cm^{-1}) because of the similar core arrangement and bridging angles in the dinuclear units of **3** (**3a,b**) and **1**. Likewise, J_2 is also expected to be positive due to the value of the Ni−O−Ni

(26) Bu, X.-H.; Du, M.; Zhang, L.; Liao, D.-Z.; Tang, J.-K.; Zhang, R.-H.; Shionoya, M. *J. Chem. Soc., Dalton Trans.* **2001**, 593.

(27) Escuer, A.; Font-Bardía, M.; Kumar, S. B.; Solans, X.; Vicente, R. *Polyhedron* **1999**, *18*, 909.

(28) The series of calculations were made using the computer program CLUMAG which uses the irreducible tensor operator formalism (ITO): Gatteschi, D.; Pardi, L. *Gazz. Chim. Ital.* **1993**, *123*, 231.

Scheme 4

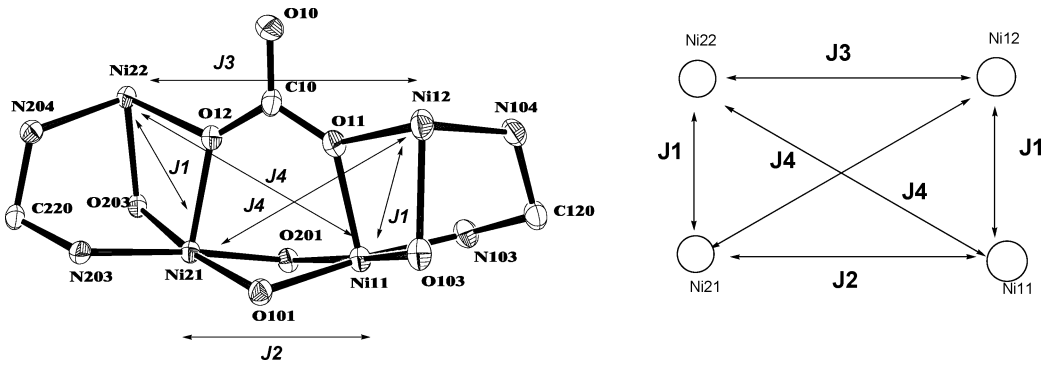

angles, close to 90° (Ni11−O101−Ni21 and Ni11−O201−Ni21 angles of 91.30 and 93.30°, respectively).[25,26] Finally, J_3 and J_4 are assigned to the cross-link interactions through the μ_4-η^2:η^2-O,O carbonate donor. As mentioned above, this type of coordination mode of the carbonate ligand is highly unusual and, to the best of our knowledge, it has not been magnetically characterized until now. Despite this, the magnitude of these interactions could be predicted by comparison with those of other related carbonate complexes. Accordingly, J_3 and J_4 are expected to be small compared with J_1 and J_2,[11] as they correspond to four-bond connection interactions, whereas J_1 and J_2 are associated with more direct two-bond magnetic pathways.

Conclusions

The dinuclear nickel complex **1**·2H_2O spontaneously reacts with CO_2 from air in a basic medium to yield the carbonate complex **3**·1.5MeOH·MeCN·H_2O in a self-assembly process. The crystal structure of **3** shows some unusual features. Accordingly, **3** presents a scarcely related μ_4-η^2:η^2-O,O carbonate ligand, not reported for the first-row transition metal complexes until now, as well as an unfamiliar coordination mode for the external phenol arms of the Schiff base ligand.

The magnetic characterization of **1**·2H_2O shows an intramolecular ferromagnetic coupling, ascribed to the countercomplementary effect of the oxygen bridges and the NCN link provided by the Schiff base.[11] Thus, this ligand seems to easily yield dinuclear complexes with a predefined $S = 2$ ground state that can act as building blocks in the isolation of compounds with a larger spin pair. The magnetic study of the tetranuclear cluster **3**·1.5MeOH·MeCN·H_2O, constructed from the dinuclear block **1**·2H_2O and the μ_4-η^2:η^2-O,O carbonate cross-link, appears to agree with this scheme. Accordingly, **3**·1.5MeOH·MeCN·H_2O constitutes the first μ_4-η^2:η^2-O,O carbonate complex magnetically characterized, and it shows an overall ferromagnetic behavior with an $S = 4$ ground state. This result must be highlighted: the dinucleating Schiff base induces a ferromagnetic coupling per se between the metal centers allocated in each one of its N_2O_2 pockets; these dinuclear units can act as initial building blocks in the construction of transition metal clusters of larger S ground states by the use of appropriate linking donors, as it seems to emerge from this report. Further studies are in due course to isolate high-nuclearity complexes with greater spin ground states.

Acknowledgment. We thank Xunta de Galicia (PGIDT03-XIB20901PR) for financial support.

Supporting Information Available: Crystallographic data for complexes **1**·3MeCN·2H_2O, **2**·2.25MeCN·H_2O, and **3**·1.5MeOH·MeCN·H_2O in CIF format and Figures S1 and S2. This material is available free of charge via the Internet at http://pubs.acs.org.

IC051194S